A Novel Approach to Monodisperse, Luminescent Silica Spheres

Adam M. Jakob and Thomas A. Schmedake*

Department of Chemistry, University of North Carolina, Charlotte, NC 28223

Received March 20, 2006
Revised Manuscript Received June 2, 2006

We report a new class of monodisperse, luminescent silica spheres produced upon calcination of hybrid aminopropyl-silica spheres (Figure 1). The optical properties of the luminescent spheres (refractive index, absorbance, and fluorescence) depend on the quantity of (aminopropyl)-triethoxysilane (APTES) in the precalcined material. This provides a "one-pot" process for growing gram-scale quantities of tailorable, brightly luminescent, monodisperse silica spheres under basic conditions without the subsequent addition of inorganic or organic fluorophores.

Although crystalline silica does not luminesce in the visible region upon exposure to UV light, silica grown via acid-catalyzed sol−gel processes often exhibits a broad-band luminescence.[1] The luminescence is especially strong and tailorable when organic acids are used during sol−gel formation (quantum yields as high as 35%).[2] Unfortunately, basic conditions are required to generate smooth, submicrometer, monodisperse silica spheres from the condensation of tetraethyl orthosilicate (TEOS) via the Stöber−Fink−Bohn (SFB) process.[3] SFB spheres are not luminescent; consequently, much research has focused on various methods of doping them with fluorophores. Common organic fluorophores have been attached through condensation reactions with APTES-functionalized silica spheres.[4] Incorporation of inorganic emission centers into SFB spheres has been demonstrated with lanthanides[5,6] and quantum dots.[7] Most of these procedures unfortunately require multiple processing steps and use expensive and/or toxic fluorophores. The attractive combination of size-control, monodispersity, surface smoothness, and luminescence continues to drive this area of research and has enabled a broad array of applications. Luminescent, monodisperse silica spheres have been used recently in chemical sensing,[8] nerve-agent detection,[9] bioanalytical assays,[10] blood-flow monitoring,[7] and in photonic crystals/synthetic opals.[11]

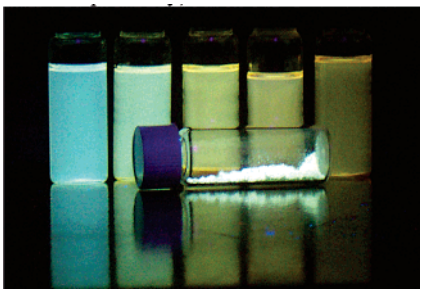

Figure 1. Luminescent silica spheres excited with a 365 nm lamp (background (L to R): **S3**, **S8**, **S20**, **S29**, **S49** suspended in ethanol; foreground: solid **S3**).

In our study, a series of aminopropylsilica spheres were synthesized in a procedure similar to that of van Blaaderen and Vrij.[12] In a typical synthesis (that for sample **S3**), ethanol (49.5 mL) was added to a 100 mL round-bottom flask, along with a magnetic stir bar. Concentrated ammonium hydroxide solution (2.0 mL) and water (6.3 mL) were added and stirred at 700 rpm. TEOS (2.23 mL, 9.95 mmol) and APTES (0.07 mL, 0.298 mmol) were added at the same time and stirred overnight.The resulting colloidal suspension was filtered through a 200 nm membrane filter, and the precipitate was rinsed with ethanol (95%) at least three times. The spheres were then dried and subsequently calcined in a tube furnace in air at 400 °C for 2 h. Calcined spheres were then washed three times with ethanol in an ultrasonic bath. The ratio of TEOS to APTES was varied while keeping the net volume of silica precursor constant (2.3 mL, nom. 10 mmol). A series of six samples was synthesized following this general procedure **S0**, **S3**, **S8**, **S20**, **S29**, and **S49** (mol % APTES = 0, 2.9, 7.5, 20, 29, and 49%, respectively).

SEM images of the spheres after being heated in air at 400 °C for 2 h (Figure 2) show nearly monodisperse spheres with a relative standard deviation below 10% for all six samples.[13] Varying the APTES concentration had noticeable effects on the structural properties of the spheres. Particle size appears to be inversely related to the percent APTES concentration (Figure 3). Surface roughness also increased with percent APTES concentration, particularly after calcination. For APTES concentrations much greater than 49 mol %, no spheres were observed in the SEM.

Index-matching experiments confirm that the refractive index increases with increasing APTES concentration (Figure 4), consistent with observations by van Blaaderen and Vrij.[12] The percent transmittance of a colloidal suspension (0.5 wt

* To whom correspondence should be addressed. E-mail: tschmeda@uncc.edu.

(1) Yoldas, B. E. *J. Mater. Res.* **1990**, *5*, 1157.
(2) Green, W. H.; Le, K. P.; Grey, J.; Au, T. T.; Sailor, M. J. *Science* **1997**, *276*, 1826.
(3) Stöber, W.; Fink, A.; Bohn, E. *J. Colloid Interface Sci.* **1968**, *26*, 62.
(4) van Blaaderen, A.; Vrij, A. *Langmuir* **1992**, *8*, 2921.
(5) Sloof, L. H.; de Dood, M. J. A.; van Blaaderen, A.; Polman, A. *Appl. Phys. Lett.* **2000**, *76*, 3682.
(6) Zhao, D.; Qin, W.; Wu, C.; Qin, G.; Zhang, J.; Lü, S. *Chem. Phys. Lett.* **2004**, *388*, 400.
(7) Chan, Y.; Zimmer, J. P.; Stroh, M.; Steckel, J. S.; Jain, R. K.; Bawendi, M. G. *Adv. Mater.* **2004**, *16*, 2092.
(8) Zhang, P.; Guo, J. H.; Wang, Y.; Pang, W. Q. *Mater. Lett.* **2002**, *53*, 400.
(9) Kim, T. H.; Li, G.; Park, W. H.; Lee, T. S. *Mol. Cryst. Liq. Cryst.* **2006**, *445*, 185.
(10) Rossi, L. M.; Shi, L.; Quina, F. H.; Rosenzweig, Z. *Langmuir* **2005**, *21*, 4277.
(11) Bogomolov, V. N.; Gaponenko, S. V.; Germanenko, I. N.; Kapitonov, A. M.; Petrov, E. P.; Gaponenko, N. V.; Prokofiev, A. V.; Ponyavina, A. N.; Silvanovich, N. I.; Samoilovich, S. M. *Phys. Rev. E* **1997**, *55*, 7619.
(12) van Blaaderen, A.; Vrij, A. *J. Colloid Interface Sci.* **1993**, *156*, 1.
(13) SEM experiments were performed on a field emission scanning emission electron microscope (Raith 150 with a Leo Gemini column). SEM images were typically acquired at 10 kV without gold sputtering. Average particle size and standard deviation was determined by imaging 20 random spheres. Confidence intervals were calculated at a 95% confidence level using a *t* value of 2.093.

10.1021/cm060664t CCC: $33.50
Published on Web 06/14/2006

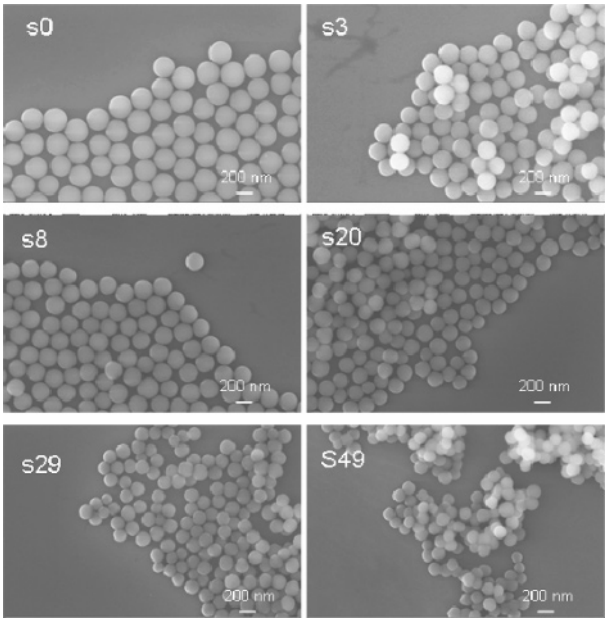

Figure 2. Calcined spheres imaged at 30 000× magnification by a field emission scanning emission electron microscope (Raith 150 with a Leo Gemini column). SEM images were acquired at 10 kV, with the low voltage allowing silica spheres to be imaged without gold sputtering.

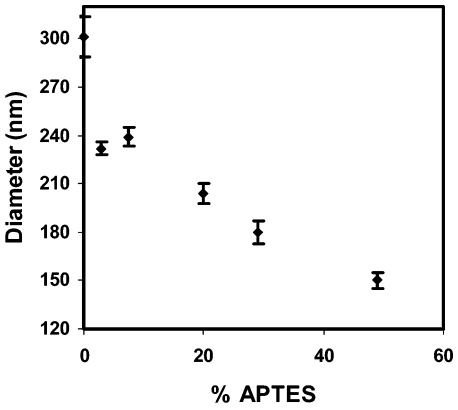

Figure 3. Diameter of spheres determined by SEM images. Bars indicate 95% confidence interval.

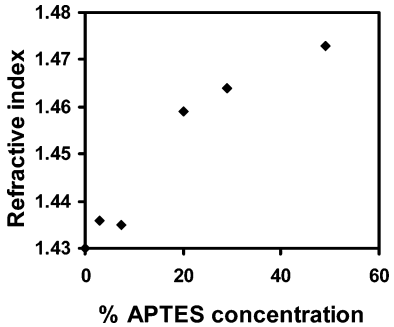

Figure 4. Refractive index of calcined spheres as a function of the original mol % APTES.

% spheres) in a 90/10 toluene/ethanol solution (n_D solvent = 1.4788) was measured at 589 nm (sodium D line). Gradually, a 0.5 wt % sample of spheres in 100% ethanol (n_D = 1.3600) was added to the scattering solution while the percent transmission was monitored continuously using a Cary 300 Bio UV−vis spectrometer. The maximum percent transmittance corresponds to the point at which the refractive index of the spheres and the refractive index of the solvent

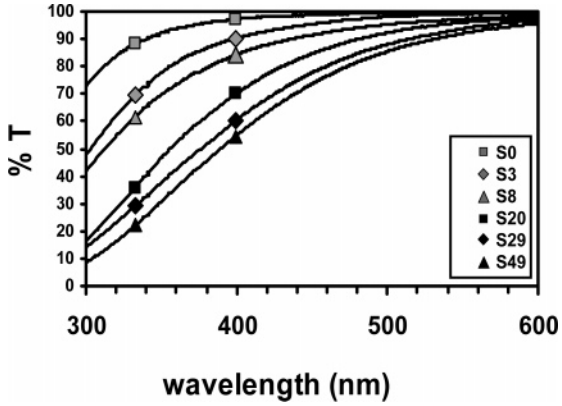

Figure 5. UV−vis percent transmittance of 0.5 wt % sphere samples in solvent index matched at 589 nm.

system are matched. This simple index matching model does not account for preferential adsorption effects from the mixed solvent system, but because the spheres are approximately 300 nm in diameter, preferential adsorption effects are expected to be relatively small. It should be noted that the refractive index of silica spheres is largely influenced by calcination temperature (SFB sphere n_D values can range from 1.38−1.46 depending on calcination temperature[14]). For consistency, all spheres were calcined under similar conditions (400 °C for 2 h).

As synthesized, the aminopropylsilica spheres appear colorless, nonfluorescent, and virtually indistinguishable from pure silica spheres. Upon calcination, the samples take on a brownish tint and a strong luminescence, both tentatively attributed to carbonaceous impurities in the silica. UV−vis transmittance measurements were obtained for 0.5 wt % samples in an ethanol/toluene solution index matched at 589 nm (Figure 5). All spectra were acquired on a Cary 300 Bio UV−vis spectrometer. The transmittance of the sphere solutions decreases with increasing APTES concentration. Qualitatively, it appears clear that scattering and absorbance are both contributing to the decreased transmittance at lower wavelengths. Further studies to quantify the absorbance and scattering of the spheres are underway. Repeated rinsing of the calcined spheres with toluene and ethanol had no effect on the transmittance, indicating that the chromophore is attached to or trapped inside the spheres. Calcination at temperatures beyond 400 °C provided colorless samples with only slightly diminished fluorescence intensity. The effects of calcination temperature and time on the optical properties of the spheres are also currently being explored.

All APTES-containing spheres were brightly luminescent after calcination, with the luminescence appearing blue to yellow as the concentration of APTES was increased. The quantum yield varies from sample to sample depending on synthesis and processing conditions, but a quantum yield as high as 12% was measured for low-doped APTES spheres calcined at 400 °C (data included in the Supporting Information). Fluorescence spectra of 0.5 wt % samples of spheres in an index-matched solution displayed different emission maxima depending on the APTES concentration (Figure 6).

(14) García-Santamaría, F.; Míguez, H.; Ibisate, M.; Meseguer, F.; López, C. *Langmuir* **2002**, *18*, 1942.

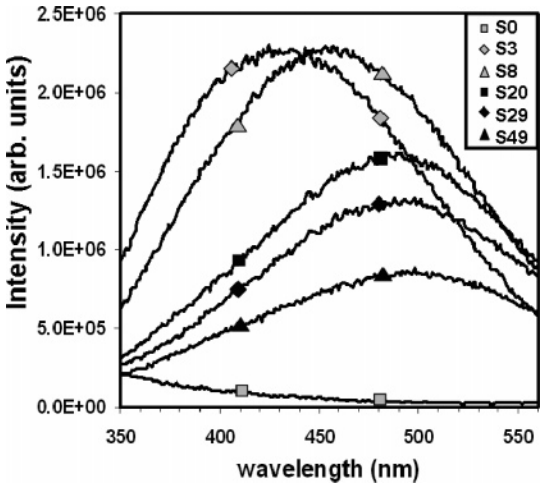

Figure 6. Emission spectra recorded on a Jobin−Yvon Fluorolog-2 fluorescence spectrometer. Samples were excited at 300 nm with 2 nm band-pass slit widths.

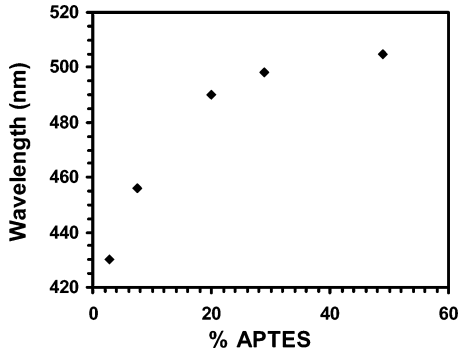

Figure 7. Fluorescence maximum as a function of APTES concentration.

Silica spheres grown without any APTES present (**S0**) display no fluorescence at room temperature. Spheres grown with 3% APTES (**S3**) emitted with a $\lambda_{max} = 430$ nm and a fwhm ≈ 150 nm. The emission maximum red-shifted with increasing APTES concentration, approaching an upper limit around 505 nm ($\lambda_{max} = 430$ nm, **S3**; 456 nm, **S8**; 490 nm, **S20**; 498 nm, **S29**; and 505 nm, **S49** (Figure 7).

The origin of the luminescence in these modified SFB spheres grown under basic conditions is tentatively assigned to the introduction of carbon and oxygen defects in the silica network resulting from calcination of the aminopropyl groups. This assignment is on the basis of comparison to the much-studied luminescent sol−gels derived from condensation of TEOS, tetramethyl orthosilicate (TMOS), or APTES with organic acids.[22] Luminescence in acid-condensed silica sol−gels has been generally attributed to defect centers in the silica[1], carbon/oxygen impurities[2], nitrogen centered effects,[15,16] and/or charge-transfer mechanisms.[17] A charge-transfer mechanism between silicon and oxygen atoms in the silica has been proposed for the observed blue emission in aged TEOS and sol−gels derived from aged TEOS.[17] This mechanism can be discounted in our SFB spheres grown from freshly distilled organosilica precursors because the APTES-free spheres, **S0**, do not exhibit fluorescence when excited at 300 nm. Mechanisms involving NH_2 centers[16] and nitrogen-rich nanodomains[15] have been developed to explain the visible luminescence resulting from some aminosols without heat activation. This is doubtful in our case, because the APTES-containing spheres do not fluoresce until after being heated to 400 °C. Our results are consistent with a carbon/oxygen-related defect center mechanism resulting from calcination of the APTES-containing spheres. Further experiments are underway to explore the effects of calcination conditions and elucidate the origin and wavelength variation of the luminescence.

Acknowledgment. This research was sponsored by a Research Corporation Cottrell College Science Award CC5902. The investigators also gratefully acknowledge the personnel support generously provided by the Thomas Walsh Tuition Fellowship and also DARPA Grant W911NF-04-1-0319 via a collaborative research agreement with ARL/SEDD.

Supporting Information Available: Index-matching data, SEM images of precalcined spheres, and quantum yield determination data. This material is available free of charge via the Internet at http://pubs.acs.org.

CM060664T

(15) Brankova, T.; Bekiari, V.; Lianos, P. *Chem. Mater.* **2003**, *15*, 1855.
(16) Carlos, L. D.; Sá Ferreira, R. A.; Pereira, R. N.; Assunção, M.; de Zea Bermudez, V. *J. Phys. Chem. B* **2004**, *108*, 14924.
(17) García, J.; Mondragón, M. A.; Téllez, C.; Campero, A.; Castaño, V. M. *Mater. Chem. Phys.* **1995**, *41*, 15.